Use of a nondirect-product basis for treating singularities in triatomic rotational–vibrational calculations

Gábor Czakó,[a] Tibor Furtenbacher,[a] Paolo Barletta,[ab] Attila G. Császár,[a] Viktor Szalay[c] and Brian T. Sutcliffe[d]

A technique has been developed which in principle allows the determination of the full rotational–vibrational eigenspectrum of triatomic molecules by treating the important singularities present in the triatomic rotational–vibrational kinetic energy operator given in Jacobi coordinates and the R_1 embedding. The singular term related to the diatom-type coordinate, R_1, deemed to be unimportant for spectroscopic applications, is given no special attention. The work extends a previous [*J. Chem. Phys.*, 2005, **122**, 024101] vibration-only approach and employs a generalized finite basis representation (GFBR) resulting in a nonsymmetric Hamiltonian matrix [*J. Chem. Phys.*, 2006, **124**, 014110]. The basis set to be used is obtained by taking the direct product of a 1-D DVR basis, related to R_1, with a 5-D nondirect-product basis, the latter formed by coupling Bessel-DVR functions depending on the distance-type coordinate causing the singularity, associated Legendre polynomials depending on the Jacobi angle, and rotational functions depending on the three Euler angles. The robust implicitly restarted Arnoldi method within the ARPACK package is used for the determination of a number of eigenvalues of the nonsymmetric Hamiltonian matrix. The suitability of the proposed approach is shown by the determination of the rotational–vibrational energy levels of the ground electronic state of H_3^+ somewhat above its barrier to linearity. Convergence of the eigenenergies is checked by an alternative approach, employing a Hamiltonian expressed in Radau coordinates, a standard direct-product basis, and no treatment of the singularities.

I. Introduction

Although strategies and codes applicable not only to the three-,[1] but to the four-,[2–6] five-,[7] and even six-atomic[8] variational (ro)vibrational problems have appeared, many of these exact approaches can be employed efficiently only for the lower end of the full spectrum. This presents a considerable problem as there is significant interest in high-lying states which are hardly amenable to experiments but should be possible to determine with the sophisticated techniques of molecular quantum mechanics (see, *e.g.*, ref. 9–11). Theoretical techniques that do not treat the singularities occurring[12] in the rotational–vibrational Hamiltonians may result in sizeable errors for some of the higher-lying rovibrational wave functions which depend on coordinates characterizing the singularity. Even though such singularities are not actually physical, they can have practical implications. They arise because it is not possible mathematically to separate rotational motion from internal motion without transforming to a coordinate system in which, in some region, the Jacobian of the transformation vanishes, leading to singularities in the Hamiltonian when expressed in the system coordinates. If a singular region contains a configuration of physical interest, it cannot be described with such a coordinate choice. It is however often possible to choose a transformation in which the Jacobian vanishes only in regions which are physically inaccessible in the energy range of interest. Thus, the choice of coordinates, though mathematically arbitrary, and the related choice of basis functions do have physical and computational consequences. In certain practical applications it may be possible to avoid the consequences of singularities by appropriate coordinate choices and/or suitable computational protocols; for examples, see ref. 2 and 13–17. Results obtained with variational procedures which are able to determine accurate rotational–vibrational eigenenergies up to the dissociation limit(s) of the related potential energy surfaces (PESs) are still relatively scarce.[18–22] The most efficient codes employ variants of the discrete variable representation (DVR) technique[23–27] and the related quadrature approximation,[25,28,29] and for triatomic species the use of rovibrational Hamiltonians expressed in orthogonal coordinates[30] has become widespread.[28,31,32]

As to vibrational ($J = 0$) triatomic Hamiltonians in internal coordinates, different strategies have been developed for treating the singularities characterizing them. Henderson *et al.*[15] combined a direct-product basis with an analytic formula to calculate the matrix elements of the R_2^{-2}-dependent part of the

[a] *Laboratory of Molecular Spectroscopy, Institute of Chemistry, Eötvös University, P. O. Box 32, H-1518 Budapest 112, Hungary*
[b] *Department of Physics and Astronomy, University College London, Gower Street, London, UK WC1E 6BT*
[c] *Crystal Physics Laboratory, Research Institute for Solid State Physics and Optics, Hungarian Academy of Sciences, P. O. Box 49, H-1525 Budapest, Hungary*
[d] *Service de Chimie Quantique et Photophysique, Université Libre de Bruxelles, B-1050 Bruxelles, Belgium*

This journal is © the Owner Societies 2007

Phys. Chem. Chem. Phys., 2007, **9**, 3407–3415 | 3407

Sutcliffe–Tennyson kinetic energy operator [see eqn (1b) below] by using spherical oscillator functions[33] and extra transformations. Watson[14] advocated the use of hyperspherical coordinates[34] to avoid the radial singularity problem. Bramley et al.[20] advocated the use of a nondirect product basis with a Jacobi Hamiltonian within a pseudospectral Lanczos algorithm. Mandelshtam and Taylor[21] advanced a simple and efficient direct-product DVR procedure made suitable to treat the singularity numerically by symmetrization of the sinc-DVR basis employed and use of an angular momentum cutoff. A simple and efficient regularization technique advocated by Baye et al.[35] can also be used to treat terms singular in the Hamiltonian during grid-based variational calculations. This approach has been employed to treat the radial singularities present in three-body vibrational Hamiltonians employing model potentials (harmonic, Gaussian, and Coulomb potentials).[36]

If the radial and angular singularities present in the kinetic energy operator are coupled, an optimal basis is always a nondirect product of the functions of the coupled coordinates. Nevertheless, to the best of our knowledge, there are only two techniques available that treat the singularities using a nondirect-product basis. Bramley et al. (BTCC)[20] advocated an approach that treats the radial singularity in a triatomic vibrational problem by using 2-D nondirect-product polynomial basis functions, which are the analytic eigenfunctions of the spherical harmonic oscillator Hamiltonian. In 2005 some of the authors of this study published[37] a similar nondirect-product basis method employing a generalized finite basis representation (GFBR) method[27,38] for the triatomic vibrational problem, whereby Bessel-DVR functions, developed by Littlejohn and Cargo,[39] were coupled to Legendre polynomials. These basis functions are not polynomials; therefore, a standard Gauss quadrature could not be used to determine the potential energy matrix. The same authors later[40] much improved their technique for computing the elements of the potential energy matrix (see also below).

As briefly, and perhaps incompletely, summarized, various techniques have been developed to solve the radial singularity problem occurring in variational vibrational computations. Again, to the best of our knowledge methods have not yet appeared that treat all the important radial singularities in the full 6-D rotational–vibrational Hamiltonian of triatomic molecules using nondirect-product bases. Therefore, the work described here had been executed with three particular aims in mind. First, we wanted to extend our nondirect-product technique[37] and code based on Bessel-DVR functions and GFBR so that it could be used to obtain the full rotational–vibrational eigenspectrum of triatomic molecules. Second, recognizing that determination of a large number of eigenvalues of large nonsymmetric Hamiltonians is a nontrivial problem, we wanted to test the utility of the implicitly restarted Arnoldi technique,[41] as implemented in the ARPACK package,[42] to obtain a desired set of rotational–vibrational eigenenergies. At the same time, the use of a non-polynomial nondirect-product basis is a good test of the GFBR methods. Third, a particularly straightforward test of the algorithm is offered by computing rotational–vibrational energy levels of X_3 species, H_3^+ in this paper, somewhat above their barrier to

linearity. Convergence of the eigenvalues in the case of H_3^+ can be checked with a particularly simple direct-product DVR computation[31,32] utilizing the orthogonal Radau coordinates.[43] The advantage of the Radau coordinates is that they minimize the problem of a radial coordinate going to zero with low-energy linear structures. Of course, the Radau coordinate Hamiltonian is not devoid of the singularity problem but it shows up only at considerably higher energies. Convergence characteristics and computer resource utilization of the drastically different approaches used to determine rotational–vibrational eigenenergies of H_3^+ allow for interesting and useful comparisons.

II. Algorithmic details

A. Coordinate system, Hamiltonian, and basis functions

Singularities will always be present in an internal coordinate rotational–vibrational Hamiltonian expressed in a rotating body-fixed frame.[12] The number and type of singularities depend on the choice of the internal coordinate system and the embedding of the axis system chosen. In the orthogonal Jacobi coordinate system, the coordinate R_1 is the diatomic distance, R_2 is the separation of the third atom from the center of mass of the diatom, and Θ is the enclosed angle. The singularity associated with R_1 (eqn (1), vide infra) occurs for the nuclear coalescence point of the diatom, which is a physically irrelevant region for rovibrational computations because the potential energy value is going to be infinite and the wave function tends to vanish there. For this reason it is clearly advantageous to choose for the z-axis of the molecule-fixed frame to lie along the R_1 coordinate, called the R_1 embedding.[30] In this embedding the molecular plane is perpendicular to the y-axis. The rovibrational Hamiltonian of a triatomic molecule in Jacobi coordinates (R_1, R_2, Θ) and employing the R_1 embedding is given in atomic units as[30,44]

$$\hat{H}_{\text{rot-vib}} = \hat{T} + \hat{V} = \hat{T}_{\text{vib}} + \hat{T}_{\text{rot-vib}} + \hat{V}, \quad (1a)$$

$$\hat{T}_{\text{vib}} = -\frac{1}{2\mu_1}\frac{\partial^2}{\partial R_1^2} - \frac{1}{2\mu_2}\frac{\partial^2}{\partial R_2^2} - \left(\frac{1}{2\mu_1 R_1^2} + \frac{1}{2\mu_2 R_2^2}\right)$$
$$\times \left(\frac{\partial^2}{\partial \Theta^2} + \cot\Theta\frac{\partial}{\partial \Theta} - \frac{\hat{j}_z^2}{\sin^2\Theta}\right), \quad (1b)$$

$$\hat{T}_{\text{rot-vib}} = \frac{1}{2\mu_1 R_1^2}(\hat{J}^2 - 2\hat{J}_z\hat{j}_z - \hat{J}_+\hat{j}_- - \hat{J}_-\hat{j}_+) \quad (1c)$$

where μ_1 and μ_2 are the usual reciprocal reduced masses, the volume element of integration is taken as $dR_1 dR_2 d(\cos\Theta)$, $\hat{J}$ is the total angular momentum, and $\hat{j}$ refers to the rotational angular momentum of the diatom.

$\hat{T}$ has three singularities, at $R_1 = 0$, at $R_2 = 0$, and at $\sin\Theta = 0$. As has been emphasized repeatedly, the $R_1 = 0$ singularity needs no special attention. The Θ-dependent part of eqn (1b) is always singular if the molecule vibrates to the linear geometry or, in a more technical sense, if the basis functions sample the linear geometry. This $\sin\Theta = 0$ singularity does not mean generally that R_2 is also zero. However, the $R_2 = 0$ singularity is coupled with the angular singularity,

because if R_2 is zero then Θ becomes undefined. Therefore, in the Jacobi coordinate system one should use[20] a 2-D $\{R_2, \Theta\}$ nondirect-product basis for treating the radial singularity in R_2 which is coupled with the angular singularity.

The full 6-D basis function with angular momentum J, parity p [$p = (0/1)$ corresponds to (odd/even)], and the usual quantum numbers $M = |m|$ and $K = |k|$, corresponding to space-fixed and body-fixed projections of the rotational angular momentum on the z axis, can be written as

$$\Phi_{n_1,n_2,\ell}^K(R_1, R_2, \Theta)C_{MK}^{Jp}(\varphi, \chi, \psi). \tag{2}$$

In eqn (2) $C_{MK}^{Jp}(\varphi, \chi, \psi)$ is the rotation function (parity-adapted symmetric-top eigenfunctions), which depends on the three Euler angles defining the orientation of the body-fixed frame with respect to the laboratory frame.

The function $\Phi_{n_1,n_2,\ell}^K(R_1, R_2, \Theta)$ is taken as the product of a 1-D DVR basis $\{\chi_{n_1}(R_1)\}$ with a Bessel-DVR set $\{F_{\ell n_2}(R_2)\}$ times an associated Legendre polynomial set $\{P_\ell^K(\cos\Theta)\}$:

$$\Phi_{n_1,n_2,\ell}^K(R_1, R_2, \Theta) = \chi_{n_1}(R_1)F_{\ell n_2}(R_2)P_\ell^K(\cos\Theta). \tag{3}$$

The index ℓ couples the associated Legendre polynomials to the Bessel-DVR functions, which are defined as

$$F_{\ell n_2}(R_2) = (-1)^{n_2+1}\frac{\sqrt{K_v}z_{vn_2}\sqrt{2z}}{z^2 - z_{vn_2}^2}J_v(z) \tag{4}$$

where $z = K_v R_2$, $K_v = z_{vN_2}/R_v^{\max}$, z_{vn_2} is the n_2th zero of the Bessel function of fractional order $J_v(z)$, and $v = \ell + \frac{1}{2}$. The set of Bessel grid points is defined as $r_{\ell n_2} = z_{vn_2}/K_v$, thus all the grid points are in the interval $0 < r_{\ell n_2} \leq R_v^{\max}$. The v-dependent $R_v^{\max}$ is a free parameter used to define the range of the R_2 coordinate.

The size of the basis set in an actual calculation is defined as follows. The number of R_1-dependent functions is N_1. The total number of Bessel-DVR functions is N_2 for each ℓ and the number of associated Legendre polynomials is L for each K. The index ℓ is set to run from K to $K + L - 1$. K goes from 0 to J, with the exception of the even-parity functions, where the $K = 0$ rotation function does not exist. The size of the total 6-D basis is therefore $N_1N_2L(J + 1 - p)$. The r_{k_1} radial points are defined for the R_1-dependent functions, whereas for each K a set of L angular Gaussian quadrature points q_k^K is defined corresponding to the set of P_ℓ^K associated Legendre polynomials. Therefore, the size of the angular grid is $L(J + 1 - p)$.

B. The kinetic energy matrix

The matrix representation of $\hat{T}_{\text{vib}}$, starting with the integral over the angular coordinates, is

$$\langle P_\ell^K C_{MK}^{Jp}|\hat{T}_{\text{vib}}|P_{\ell'}^{K'}C_{MK'}^{Jp}\rangle = \hat{T}_\ell^{(1)}\delta_{\ell,\ell'}\delta_{K,K'} + \hat{T}_\ell^{(2)}\delta_{\ell,\ell'}\delta_{K,K'}, \tag{5}$$

where

$$\hat{T}_\ell^{(j)} = -\frac{1}{2\mu_j}\frac{\partial^2}{\partial R_j^2} + \frac{1}{2\mu_j R_j^2}\ell(\ell + 1) \tag{6}$$

and $j = 1$ or 2.

The matrix elements of the R_1-dependent $\hat{T}_\ell^{(1)}$ operator are computed as

$$(\boldsymbol{T}_\ell^{(1)})_{n_1,n_1'} = (\boldsymbol{T}^{(1)})_{n_1,n_1'} + (\boldsymbol{R}_1^{-2})_{n_1,n_1'}\ell(\ell + 1), \tag{7}$$

where the matrix elements of the corresponding differential operator,

$$(\boldsymbol{T}^{(1)})_{n_1,n_1'} = \left\langle \chi_{n_1}(R_1)| -\frac{1}{2\mu_1}\frac{\partial^2}{\partial R_1^2}|\chi_{n_1'}(R_1)\right\rangle, \tag{8}$$

can be obtained by exact analytical formulae.[45] The DVR representation of the R_1^{-2} part of the kinetic energy operator matrix is calculated using the quadrature approximation and the radial points r_{n_1} as

$$(\boldsymbol{R}_1^{-2})_{n_1,n_1'} = \left\langle \chi_{n_1}(R_1)|\frac{1}{2\mu_1 R_1^2}|\chi_{n_1'}(R_1)\right\rangle \cong \frac{1}{2\mu_1 r_{n_1}^2}\delta_{n_1,n_1'}. \tag{9}$$

As to the R_2-dependent $\hat{T}_\ell^{(2)}$ operator, we avoid using the quadrature approximation for computing its matrix elements in order to treat the R_2^{-2} singularity. The matrix elements of $\hat{T}_\ell^{(2)}$,

$$(\boldsymbol{T}_\ell^{(2)})_{n_2,n_2'} = \left\langle F_{\ell n_2}(R_2)|\hat{T}_\ell^{(2)}|F_{\ell n_2'}(R_2)\right\rangle, \tag{10}$$

are evaluated using an analytical formula taken from ref. 37 and 39.

Employing eqns (7) and (10), the DVR/FBR representation of $\hat{T}_{\text{vib}}$ is written as

$$(\boldsymbol{T}_{\text{vib}})_{n_1n_2\ell K,n_1'n_2'\ell'K'} = (\boldsymbol{T}_\ell^{(1)})_{n_1,n_1'}\delta_{n_2,n_2'}\delta_{\ell,\ell'}\delta_{K,K'} + \delta_{n_1,n_1'}(\boldsymbol{T}_\ell^{(2)})_{n_2,n_2'}\delta_{\ell,\ell'}\delta_{K,K'}. \tag{11}$$

For the matrix representation of $\hat{T}_{\text{rot-vib}}$ one takes advantage of the properties of the $C_{MK}^{Jp}(\varphi, \chi, \psi)$ rotational functions. The matrix representation of $\hat{T}_{\text{rot-vib}}$ is

$$(\boldsymbol{T}_{\text{rot-vib}})_{n_1n_2\ell K,n_1'n_2'\ell'K'} = (\tilde{\boldsymbol{R}}_1^K)_{n_1,n_1'}\delta_{n_2,n_2'}\delta_{\ell,\ell'}\delta_{K,K'}$$
$$+ (\tilde{\boldsymbol{R}}_1^{-2})_{n_1,n_1'}\delta_{n_2,n_2'}(\boldsymbol{B}_K^+)_{\ell,\ell'}\delta_{K+1,K'}$$
$$+ (\tilde{\boldsymbol{R}}_1^{-2})_{n_1,n_1'}\delta_{n_2,n_2'}(\boldsymbol{B}_K^-)_{\ell,\ell'}\delta_{K-1,K'}, \tag{12}$$

where

$$(\tilde{\boldsymbol{R}}_1^K)_{n_1,n_1'} = \frac{J(J+1) - 2K^2}{2\mu_1 r_{n_1}^2}\delta_{n_1,n_1'}, \tag{13a}$$

$$(\boldsymbol{B}_K^\pm)_{\ell,\ell'} = -(1 + \delta_{K0} + \delta_{K\pm1,0})^{1/2}\Lambda_{JK}^\pm\Lambda_{\ell K}^\pm\delta_{\ell\pm1,\ell'}, \tag{13b}$$

and $\Lambda_{\eta K}^\pm = \sqrt{\eta(\eta + 1) - K(K \pm 1)}$.

The matrix representation of the total kinetic energy operator resulting from the combination of eqns (11) and (12) is sparse and it has a particularly simple structure. Fig. 1 shows a pictorial representation of its nonzero elements.

This journal is © the Owner Societies 2007

Phys. Chem. Chem. Phys., 2007, **9**, 3407–3415 | 3409
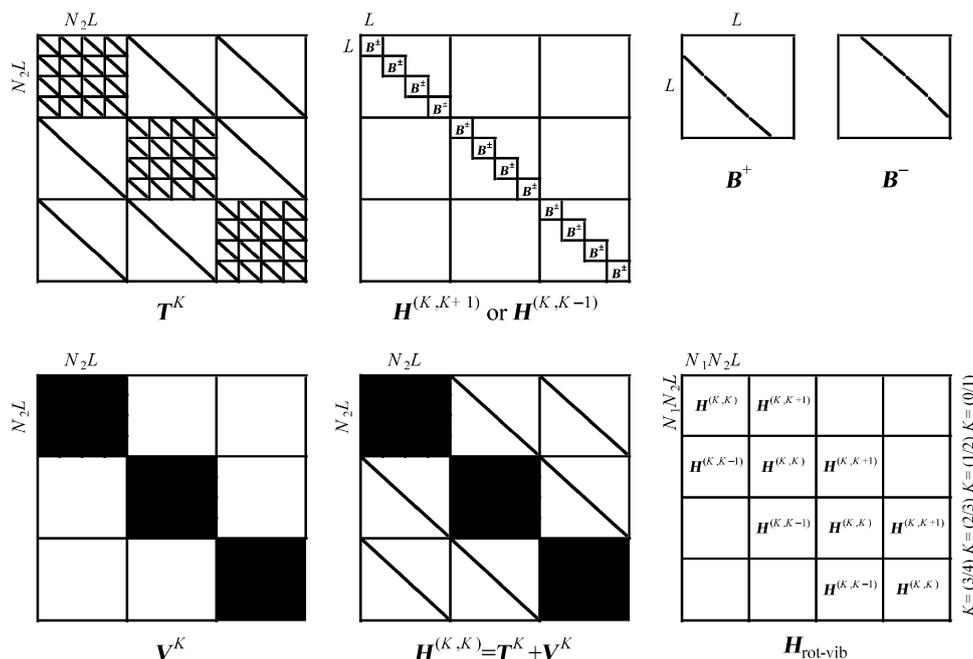
Fig. 1 Pictorial representation of the shape and the nonzero elements of the matrices appearing in eqns (20) or (21) and (22)–(25), (for the sake of clarity, $N_1 = 3$ and $N_2 = 4$). In this figure the total rovibrational Hamiltonian matrix, $\boldsymbol{H}_{\text{rot-vib}}$, is given for $J = (3/4)$ for (odd/even) parity. The matrix $\boldsymbol{B}^{\pm}$ is either the subdiagonal $\boldsymbol{B}^{+}$ or the superdiagonal $\boldsymbol{B}^{-}$ in $\boldsymbol{H}^{(K,K+1)}$ or $\boldsymbol{H}^{(K,K-1)}$, respectively.

C. The potential energy matrix

Elements of the potential energy matrix are defined as

$$
\begin{aligned}
V_{n_1 n_2 \ell K, n'_1 n'_2 \ell' K'} &= V^K_{n_1 n_2 \ell, n'_1 n'_2 \ell'} \delta_{K,K'} \\
&= \langle \Phi^K_{n_1,n_2,\ell} | V(R_1, R_2, \cos \Theta) | \Phi^K_{n'_1,n'_2,\ell'} \rangle \delta_{K,K'},
\end{aligned}
\tag{14}
$$

where advantage is taken of the fact that the potential energy operator does not depend on the Euler angles.

Since the Bessel-DVR functions are non-polynomial and in order to take advantage of a quadrature approximation, we evaluate the potential energy matrix elements by means of the generalized finite basis representation (GFBR).[40] Two methods are considered for determining the matrix representation of the potential energy operator.

Method I employs a symmetric GFBR written as

$$
\begin{aligned}
\boldsymbol{V}^K &\cong (\boldsymbol{S}^K)^{-1/2} \boldsymbol{\mathscr{V}}^K (\boldsymbol{S}^K)^{-1/2} \\
&= (\boldsymbol{S}^K)^{-1/2} \boldsymbol{\mathscr{F}}^K \boldsymbol{V}^K_{\text{diag}} (\boldsymbol{\mathscr{F}}^K)^{+} (\boldsymbol{S}^K)^{-1/2},
\end{aligned}
\tag{15}
$$

where $\boldsymbol{S}^K = \boldsymbol{\mathscr{F}}^K (\boldsymbol{\mathscr{F}}^K)^{+}$ and

$$
(\boldsymbol{V}^K_{\text{diag}})_{k_1 \ell_2 k_2 k, k'_1 \ell'_2 k'_2 k'} = V(r_{k_1}, r_{\ell_2 k_2}, q^K_k) \delta_{k_1,k'_1} \delta_{\ell_2,\ell'_2} \delta_{k_2,k'_2} \delta_{k,k'}.
\tag{16}
$$

For each K, an $N_1 N_2 L \times N_1 N_2 L^2$-dimensional sparse rectangular matrix of special structure, $\boldsymbol{\mathscr{F}}^K$, is defined as

$$
\begin{aligned}
\boldsymbol{\mathscr{F}}^K_{n_1 n_2 \ell, k_1 \ell_2 k_2 k} &= w^{1/2}_{k_1} w^{1/2}_{\ell_2 k_2} (w^K_k)^{1/2} \chi_{n_1}(r_{k_1}) F_{\ell n_2}(r_{\ell_2 k_2}) P^K_\ell(q^K_k) \\
&= \delta_{n_1,k_1} w^{1/2}_{\ell_2 k_2} (w^K_k)^{1/2} F_{\ell n_2}(r_{\ell_2 k_2}) P^K_\ell(q^K_k),
\end{aligned}
\tag{17}
$$

where $\chi_{n_1}(r_{k_1}) = w^{-1/2}_{k_1} \delta_{n_1,k_1}$, and w_{k_1} and w^K_k are Gaussian weights. $w_{\ell_2 k_2}$ were set to 1 during the computations. The implementation of Method I involves two steps. First, the matrices $\boldsymbol{\mathscr{V}}^K$ and $\boldsymbol{S}^K$ are computed as

$$
\begin{aligned}
(\boldsymbol{\mathscr{V}}^K)_{n_1 n_2 \ell, n'_1 n'_2 \ell'} &= \sum_{k_1=1}^{N_1} \sum_{\ell_2=1}^{N_2} \sum_{k_2=1}^{L} \sum_{k=1}^{L} \boldsymbol{\mathscr{F}}^K_{n_1 n_2 \ell, k_1 \ell_2 k_2 k} \\
&\quad \times (\boldsymbol{V}^K_{\text{diag}})_{k_1 \ell_2 k_2 k, k_1 \ell_2 k_2 k} \boldsymbol{\mathscr{F}}^K_{k_1 \ell_2 k_2 k, n'_1 n'_2 \ell'} \\
&= \delta_{n_1,n'_1} \sum_{\ell_2=1}^{N_2} \sum_{k_2=1}^{L} \sum_{k=1}^{L} w_{\ell_2 k_2} w^K_k F_{\ell n_2}(r_{\ell_2 k_2}) P^K_\ell(q^K_k) \\
&\quad \times V(r_{k_1}, r_{\ell_2 k_2}, q^K_k) F_{\ell' n'_2}(r_{\ell_2 k_2}) P^K_{\ell'}(q^K_k)
\end{aligned}
\tag{18}
$$

and

$$
\begin{aligned}
(\boldsymbol{S}^K)_{n_1 n_2 \ell, n'_1 n'_2 \ell'} &= \sum_{k_1=1}^{N_1} \sum_{\ell_2=1}^{N_2} \sum_{k_2=1}^{L} \sum_{k=1}^{L} \boldsymbol{\mathscr{F}}^K_{n_1 n_2 \ell, k_1 \ell_2 k_2 k} \boldsymbol{\mathscr{F}}^K_{k_1 \ell_2 k_2 k, n'_1 n'_2 \ell'} \\
&= \delta_{n_1,n'_1} \sum_{\ell_2=1}^{N_2} \sum_{k_2=1}^{L} \sum_{k=1}^{L} w_{\ell_2 k_2} w^K_k F_{\ell n_2}(r_{\ell_2 k_2}) P^K_\ell(q^K_k) F_{\ell' n'_2}(r_{\ell_2 k_2}) P^K_{\ell'}(q^K_k).
\end{aligned}
\tag{19}
$$

Next, the expression for $\boldsymbol{V}^K$ is obtained through matrix multiplications. The explicit expression for the matrix elements is

$$
(\boldsymbol{V}^K)_{n_1 n_2 \ell, n'_1 n'_2 \ell'} = \sum_{j=1}^{N_1 N_2 L} \left(\sum_{i=1}^{N_1 N_2 L} (\boldsymbol{S}^K)^{-1/2}_{n_1 n_2 \ell, i} \boldsymbol{\mathscr{V}}^K_{i,j} \right)_{n_1 n_2 \ell, j} (\boldsymbol{S}^K)^{-1/2}_{j, n'_1 n'_2 \ell'}.
\tag{20}
$$

The $N_1 N_2 L \times N_1 N_2 L$-dimensional V^K is a block-diagonal matrix containing $N_2 L \times N_2 L$-dimensional blocks (see Fig. 1).

Method II, involving a minor modification of Method I, provides a considerably more efficient algorithm for determining V^K. The key idea[40] is that for each ℓ a set of quadrature points $\{r_{\ell k_2}\}$ can be chosen satisfying $F_{\ell n_2}(r_{\ell k_2}) = w_{\ell k_2}^{-1/2} \delta_{n_2,k_2}$, where $w_{\ell k_2}^{-1/2} = (-1)^{k_2+1}\sqrt{K_\nu z_{\nu k_2}/2} J'_\nu(z_{\nu k_2})$. There are two possible choices for the radial points $\{r_{\ell k_2}\}$, as they can be coupled to the *bra* or the *ket* of eqn (14). In eqn (21), *vide infra*, we have used the former, whereas the use of the latter would have resulted in the transpose of V^K. Then, the matrix elements are

$$
\begin{aligned}
(V^K)_{n_1 n_2 \ell, n_1' n_2' \ell'} &\cong \sum_{k_1=1}^{N_1} \sum_{k_2=1}^{N_2} \sum_{k=1}^{L} w_{k_1} w_{\ell k_2} w_k^K \chi_{n_1}(r_{k_1}) F_{\ell n_2}(r_{\ell k_2}) \\
&\quad \times P_\ell^K(q_k^K) V(r_{k_1}, r_{\ell k_2}, q_k^K) \chi_{n_1'}(r_{k_1}) F_{\ell' n_2'}(r_{\ell k_2}) P_{\ell'}^K(q_k^K) \\
&= \sum_{k_1=1}^{N_1} \sum_{k_2=1}^{N_2} \sum_{k=1}^{L} w_{k_1} w_{\ell k_2} w_k^K w_{k_1}^{-1/2} \delta_{n_1,k_1} w_{\ell k_2}^{-1/2} \delta_{n_2,k_2} \\
&\quad \times P_\ell^K(q_k^K) V(r_{k_1}, r_{\ell k_2}, q_k^K) w_{k_1}^{-1/2} \delta_{n_1',k_1} F_{\ell' n_2'}(r_{\ell k_2}) P_{\ell'}^K(q_k^K) \\
&= \delta_{n_1,n_1'} w_{\ell n_2}^{1/2} F_{\ell' n_2'}(r_{\ell n_2}) \sum_{k=1}^{L} w_k^K P_\ell^K(q_k^K) V(r_{n_1}, r_{\ell n_2}, q_k^K) P_{\ell'}^K(q_k^K).
\end{aligned}
\tag{21}
$$

It is important to note that in Method II a basis function dependent (ℓ-dependent) grid is used. Further details can be found in ref. 40. Use of Method I results in a symmetric potential energy matrix, while that of Method II in an asymmetric matrix.

D. The final Hamiltonian matrix and its eigenvalues

To set up the matrix representation of the Hamiltonian, it is useful to group the basis functions into separate sets of even and odd parity. The total Hamiltonian matrix for a given J is built up of blocks (Fig. 1), and one cycles through K to build the Hamiltonian matrix, where K also denotes the index of the cycle.

The matrix elements of the final rotational–vibrational Hamiltonian can be given as

$$
\begin{aligned}
(H_{\text{rot-vib}})_{n_1 n_2 \ell K, n_1' n_2' \ell' K'} &= (T_{\text{vib}})_{n_1 n_2 \ell K, n_1' n_2' \ell' K'} \\
&\quad + (T_{\text{rot-vib}})_{n_1 n_2 \ell K, n_1' n_2' \ell' K'} + (V^K)_{n_1 n_2 \ell, n_1' n_2' \ell'} \delta_{K,K'}.
\end{aligned}
\tag{22}
$$

Fig. 1 shows the structure of the Hamiltonian matrix, whereby

$$
\begin{aligned}
(T^K)_{n_1 n_2 \ell, n_1' n_2' \ell'} &= (T_\ell^{(1)})_{n_1,n_1'} \delta_{n_2,n_2'} \delta_{\ell,\ell'} \\
&\quad + \delta_{n_1,n_1'} (T_\ell^{(2)})_{n_2 n_2'} \delta_{\ell,\ell'} + (\tilde{R}_1^K)_{n_1,n_1'} \delta_{n_2,n_2'} \delta_{\ell,\ell'},
\end{aligned}
\tag{23}
$$

$$
(H^{(K,K\pm 1)})_{n_1 n_2 \ell, n_1' n_2' \ell'} = (R_1^{-2})_{n_1,n_1'} \delta_{n_2,n_2'} (B_K^\pm)_{\ell,\ell'},
\tag{24}
$$

and

$$
H^{(K,K)} = T^K + V^K.
\tag{25}
$$

Building the kinetic energy matrix, as compared to that of the potential energy matrix, requires almost no computer time. Therefore, to judge the cost of the computation of the Hamiltonian matrices through Methods I and II it is enough to consider the cost associated with assembling V^K. In Method I, each element of the potential matrix is computed using the same grid of $N_1 N_2 L^2$ points, which requires on the order of $N_2 L^2$ additions for each nonzero element [see eqns (18) and (19)]. In Method II, the same integral can be obtained employing only $N_1 N_2 L$ special points corresponding to the appropriate Bessel-DVR function. Furthermore, the use of the $N_1 N_2 L$ special points within Method II requires only a single summation, see eqn (21). Consequently, building the Hamiltonian matrix according to Method II is about $N_2 L$ times less expensive than that using Method I. For the largest calculations presented this means close to three orders of magnitude saving when building V^K. For Methods I and II the final symmetric or asymmetric Hamiltonian matrices have the same structure (Fig. 1). One can take advantage of the considerable sparsity and special structure of these Hamiltonian matrices by employing an iterative algorithm for the computation of the required eigenpairs or eigentriplets. Diagonalization of an asymmetric Hamiltonian matrix requires about twice as much effort as that of a symmetric matrix. For all problems of practical interest, the time-determining step of Method I is the expensive computation of the potential energy matrix, scaling as $(J + 1 - p)N_1 N_2^3 L^4$. Due to the simplification introduced in Method II, its time-determining step becomes the computation of the eigenvalues. Use of special iterative algorithms and efficient matrix-vector product evaluations during the determination of the eigenvalues makes Method II appealing for nuclear motion computations when the determination of the full rotational–vibrational spectrum is the goal, especially if the use of a nondirect-product basis results in a compact representation.

Determination of eigenenergies of a nonsymmetric matrix is not a simple task. Furthermore, given the efficient computation of the Hamiltonian matrix using Method II means that most of the computer time is spent on the determination of the eigenvalues. The relatively widely known implicitly restarted Arnoldi method,[41] whose robust implementation is available within the ARPACK package,[42] has been incorporated into our code. During the matrix-vector multiplications advantage has been taken of the sparsity and the special structure of the Hamiltonian. The implicitly restarted Arnoldi algorithm proved very stable in all test computations. For the symmetric case a local implementation[31] of the standard sparse-matrix Lanczos algorithm[46] has been used. The same algorithm was employed for the standard direct-product computations utilizing the DOPI3R code,[31,32] where DOPI stands for DVR (D) of the Hamiltonian in orthogonal (O) internal coordinates using a direct-product (P) basis followed by iterative (I) diagonalization of the resulting sparse Hamiltonian.

III. A numerial test: H_3^+

As a numerical test, rotational–vibrational energy levels of H_3^+ have been computed employing the algorithms described in section II. The global PES of H_3^+ used in these

This journal is © the Owner Societies 2007

Phys. Chem. Chem. Phys., 2007, **9**, 3407–3415 | 3411

computations is taken from ref. 47. To show the deteriorating effect of the R_2 singularity, the rotational–vibrational energy levels have also been computed by the direct-product DOPI technique.[31,32] Naturally, all these DOPI computations were performed in the Jacobi coordinate system with R_1 embedding. When using DOPI, no attempt is made to treat the important radial singularity involving R_2 so no convergence is expected for a large number of levels. In the Method I and Method II computations the R_1-dependent 1-D DVR basis set was the Hermite-DVR basis, which was also used as the R_1 and R_2 radial bases during the DOPI computations. In DOPI, associated Legendre-DVR functions have been employed for Θ. In all the tables and in the text the number of basis functions is denoted as $(N_1\ N_2\ L)$, where N_1, N_2, and L are the numbers of the R_1-, R_2-, and Θ-dependent functions, respectively.

To test the convergence of the eigenenergies obtained from Methods I and II, they need to be compared to tightly converged reference values. These have been provided by DOPI computations utilizing the Hamiltonian in orthogonal Radau coordinates. The average discrepancies, given in energy intervals, between the reference and those $J = 2$ rovibrational energy levels of H_3^+ which were computed by Methods I and II and the Jacobi-DOPI technique are given in Table 1. The results presented there can be summarized as follows:

(i) Even with small basis sets, basically the same results are obtained regardless of whether Method I or II is employed. Naturally, the two representations provide exactly the same converged eigenenergies.

(ii) The full eigenspectrum of the nonsymmetric Hamiltonian matrix from Method II can contain complex eigenvalues.

In the finite basis cases the converged or nearly converged energies are real numbers, even for the smallest, (20 20 20) case presented in Table 1. The convergence of the imaginary part of the eigenvalues to zero is much faster than the convergence of the real part.

(iii) Below the barrier to linearity, which is at about 15 000 cm^{-1} above the minimum of the PES, treatment of the singularities is not necessary. Therefore, Methods I and II and the Jacobi-DOPI algorithm give basically the same eigenenergies. As a small technicality, note that in the odd-parity case the low-lying energy levels obtained by the DOPI procedure become compromised by the radial singularity when the number of quadrature points is increased. To obtain converged results with the DOPI algorithm below the barrier to linearity, the smallest R_2 grid point has to be chosen carefully, as it has already been discussed in ref. 37.

(iv) Above the barrier to linearity, in the even-parity case the radial singularity does not come into play. Therefore, Methods I and II and DOPI give highly similar results and the eigenenergies are converging fast to their accurate values as the number of basis functions is increased.

(v) Above the barrier to linearity, it is essential to treat the R_2-dependent radial singularity present in Jacobi coordinates in the odd-parity case.

Table 2 contains selected odd-parity energy levels above the barrier to linearity. Considering the pairs $E_{231,232}$, $E_{249,250}$, $E_{251,252}$, and $E_{333,334}$, where the subscripts denote the position of the eigenenergies in the full spectrum, one component of each degenerate pair depends slightly on the radial singularity. Therefore, for this component, the Method II and DOPI results agree with each other to within 0.86 cm^{-1} in the case

Table 1 Average discrepancies in the given energy intervals between the converged and the incomplete basis set rovibrational energy levels of H_3^+ with rotational angular momentum $J = 2$, all in cm^{-1}, computed by different algortihms in the Jacobi coordinate system using the R_1 embedding[a]

Interval	Parity	(20 20 20)			(25 25 25)			(30 30 30)		
		Method I[b]	Method II[b]	DOPI[c]	Method I[b]	Method II[b]	DOPI[c]	Method I[b]	Method II[b]	DOPI[c]
0–10000	Odd	0.05	0.05	0.05	0.00	0.00	0.01	0.00	0.00	0.06
	Even	0.05	0.05	0.05	0.00	0.00	0.00	0.00	0.00	0.00
10000–11000	Odd	0.05	0.06	0.06	0.01	0.01	0.02	0.00	0.00	0.05
	Even	0.06	0.06	0.06	0.01	0.01	0.01	0.00	0.00	0.00
11000–12000	Odd	0.23	0.22	0.22	0.02	0.02	0.02	0.00	0.00	0.04
	Even	0.23	0.22	0.22	0.02	0.02	0.02	0.00	0.00	0.00
12000–13000	Odd	0.14	0.13	0.14	0.02	0.02	0.03	0.00	0.00	0.07
	Even	0.11	0.11	0.12	0.02	0.02	0.02	0.00	0.00	0.00
13000–14000	Odd	0.50	0.49	0.49	0.03	0.03	0.03	0.00	0.00	0.05
	Even	0.45	0.45	0.45	0.03	0.03	0.03	0.00	0.00	0.00
14000–15000	Odd	0.49	0.45	0.46	0.03	0.03	0.03	0.00	0.00	0.06
	Even	0.47	0.44	0.44	0.03	0.03	0.03	0.00	0.00	0.00
15000–16000	Odd	0.76	0.70	0.67	0.04	0.03	0.26	0.01	0.01	0.21
	Even	0.77	0.75	0.76	0.04	0.03	0.03	0.01	0.01	0.01
16000–17000	Odd	0.78	0.66	9.01	0.05	0.02	6.53	0.01	0.01	5.19
	Even	0.71	0.67	0.64	0.03	0.02	0.03	0.01	0.01	0.01
17000–18000	Odd	0.75	0.53	16.87	0.05	0.03	14.06	0.01	0.01	10.60
	Even	0.69	0.51	0.49	0.04	0.03	0.06	0.01	0.01	0.03
18000–19000	Odd	1.16	1.20	15.33	0.09	0.06	10.10	0.03	0.03	9.71
	Even	1.26	1.26	1.49	0.05	0.06	0.19	0.02	0.03	0.08

[a] The PES of H_3^+ is taken from ref. 47, the minimum of the PES is at $r_e(HH) = 1.64999\ a_0$. $m(H) = 1.0075372$ u is used during all the computations. All the eigenenergies refer to the minimum of the PES. The number of basis functions is given as $(N_1\ N_2\ L)$, where N_1, N_2, and L denote the number of the R_1-, R_2-, and Θ-dependent functions, respectively. [b] See text for the description of methods I and II. The R_1 Hermite-DVR grid points are in the interval [0.9, 4.5], while the radial R_2 Bessel grid ponts are in the interval $0 < r_{\ell n_2} \le 3.5 + 0.001\ (\ell + 1)$, all in a_0. [c] DOPI = results obtained with DOPI,[31,32] where the R_1 and R_2 Hermite-DVR grid points are in the intervals [0.9, 4.5] and [0.05, 3.55] a_0, respectively.

Table 2 Selected rotational–vibrational eigenenergies of H_3^+, with rotational angular momentum $J = 2$, above the barrier to linearity, all in cm^{-1}, computed by different algorithms in the Jacobi coordinate system using the R_1 embedding[a]

| No.[b]	(20 20 20)		(25 25 25)		(30 30 30)		Accurate[e]
	Method II[c]	DOPI[d]	Method II[c]	DOPI[d]	Method II[c]	DOPI[d]	
193	16215.98	16212.85	16215.07	16212.73	16215.03	16213.08	16215.04
231	17014.77	16995.59	17014.66	17000.34	17014.64	17003.08	17014.65
232	17015.47	17015.50	17014.69	17014.67	17014.65	17014.61	17014.65
249	17308.22	17293.50	17308.23	17304.25	17308.22	17305.89	17308.24
250	17308.24	17308.22	17308.27	17308.26	17308.25	17308.24	17308.24
251	17341.89	17322.97	17342.20	17335.01	17342.21	17337.86	17342.22
252	17342.64	17342.68	17342.25	17342.25	17342.22	17342.17	17342.22
315	18527.63	18528.08	18527.40	18527.19	18527.35	18527.23	18527.35
332	18738.54	18722.22	18737.97	18728.42	18737.94	18730.86	18737.96
333	18782.92	18757.26	18783.85	18773.56	18783.87	18777.15	18783.91
334	18783.46	18780.90	18783.89	18782.98	18783.90	18783.57	18783.91

[a] See footnote a of Table 1. [b] No. is the level number obtained by counting all the eigenvalues, regardless of their parity. [c] The R_1 Hermite-DVR grid points are in the interval [0.9, 4.5] and the radial R_2 Bessel grid ponts are in the interval $0 < r_{\ell n_2} \leq 3.5 + 0.001(\ell + 1)$, all in a_0. [d] See footnote c of Table 1. [e] Converged results obtained by a large DOPI computation utilizing the Radau coordinate system.

of the smallest (20 20 20) basis and the average agreement is about 0.24 and 0.11 cm^{-1} when the basis size is increased to (25 25 25) and (30 30 30), respectively. The other component depends strongly on the radial singularity; therefore, the DOPI method using Jacobi coordinates cannot yield converged eigenenergies. The average discrepancies between the accurate and the computed values are 19.93, 8.97, and 6.26 cm^{-1} employing (20 20 20), (25 25 25), and (30 30 30) basis functions, in order. Using Method II, the average errors are only 0.61 and 0.02 cm^{-1} when using the (20 20 20) and (30 30 30) bases, respectively.

There are nondegenerate energy levels where the correct treatment of the singularities is important. For example, the level E_{193} obtained by Method II is converged to within 0.94, 0.03, and 0.01 cm^{-1} using the (20 20 20), (25 25 25), and (30 30 30) bases, respectively. However, employing the DOPI method the convergence pattern is much worse; the discrepancies are 2.19, 2.31, and 1.96 cm^{-1} using the same number of basis functions. This observation emphasizes the more facile convergence characteristics of algorithms treating properly the singularities and the use of a nondirect-product basis.

Finally, a brief note concerning the accurate results referred to in Tables 1 and 2, obtained in Radau coordinates employing the exceedingly simple DOPI algorithm.[31,32] As perhaps mentioned first by Tennyson et al.,[48] in any variational calculation of the (ro)vibrational eigenspectrum of H_3^+ it is important to distinguish between the coordinate-independent barrier to linearity and the coordinate-dependent occurrence of a singularity. In the Jacobi coordinate system the radial coordinate R_2 has to be treated at and above the barrier to linearity, because R_2 becomes zero exactly when the third H atom vibrates to the center of mass of the diatom, which is by definition the barrier to linearity of H_3^+ (though not so for many of the isotopologues). This occurs when the value of the potential energy is about $10\,000$ cm^{-1} above the zero-point energy (ZPE). Consequently, many of the (ro)vibrational energy levels even just slightly above the barrier to linearity cannot be converged by a computation of reasonable size in Jacobi coordinates which does not treat the R_2 singularity. However, in Radau coordinates only the term containing sin

Θ becomes singular at the barrier. Of course, one of the radial Radau coordinates also becomes zero at a certain linear arrangement, where H_3 is about three times closer to H_1 than to H_2 (see Fig. 2 for notation). However, the lowest energy when one of the radial Radau coordinates is zero, is about $30\,000$ cm^{-1} above the ZPE (see Fig. 2). Therefore, singularities related to the radial Radau coordinates do not need special treatment during variational (ro)vibrational calculations of H_3^+ very high up on the energy ladder. This is the reason why converged rovibrational energies of H_3^+ above the barrier to linearity could be computed employing the DOPI algorithm, which does not treat the radial singularities at all. Finally, it should be noted that the (ro)vibrational Hamiltonians can be expressed in bond coordinates and due to the interatomic radial coordinates the radial singularities are shifted to physically irrelevant regions. Bond coordinates are not orthogonal; thus, the kinetic energy operator contains
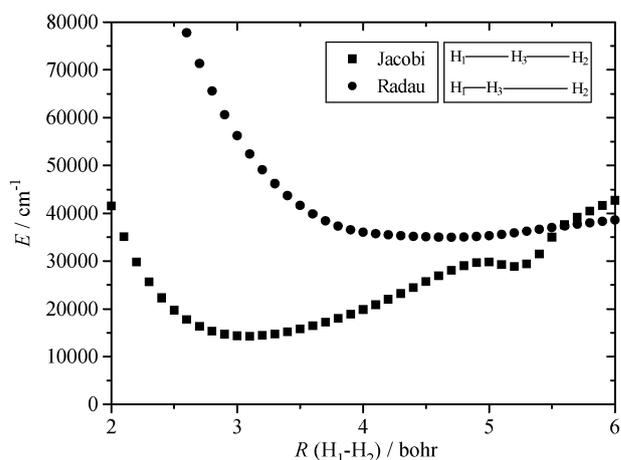
Fig. 2 Energy of onset of the radial singularity, with the PES of ref. 47, as a function of the end atom distance at linear arrangement of the three atoms of H_3^+ in Jacobi and Radau coordinates. The singular geometries occur at $R(H_1-H_3)/R(H_1-H_2) = 1/2$ and $R(H_1-H_3)/R(H_1-H_2) = 0.26794919$ in the Jacobi and Radau coordinates, respectively. The zero-point energy is at 4362.30 cm^{-1} and the first dissociation asymptote of H_3^+ is at around $37\,000$ cm^{-1}.

This journal is © the Owner Societies 2007

Phys. Chem. Chem. Phys., 2007, **9**, 3407–3415 | 3413

mixed derivatives. Furthermore, in comparision with Jacobi or Radau coordinates, bond coordinates are a poor choice for floppy molecules due to the slow convergence of the related variational procedure, as pointed out before.[2]

IV. Summary

A (pseudo)variational method, using a tailor-made nondirect-product basis, and a related computer code have been developed for treating the important radial singularities present in the triatomic rovibrational kinetic energy operator given in Jacobi coordinates in the R_1 embedding allowing, in principle, the computation of the full rotational–vibrational eigenspectrum of triatomic species. The algorithm involves application of a recently proposed[40] method for evaluating the potential energy matrix elements in the generalized finite basis representation (GFBR) required by the use of a non-polynomial nondirect-product basis. Two realizations of the GFBR procedure have been tested, Methods I and II. In Method I, resulting in a symmetric Hamiltonian matrix, each element of the potential matrix V^K is computed using the same grid of $N_1 N_2 L^2$ points, which requires additions for each nonzero element on the order of $N_2 L^2$ [see eqns (18) and (19)]. In Method II, resulting in a nonsymmetric Hamiltonian matrix, the same integral is obtained employing only $N_1 N_2 L$ special points corresponding to the appropriate Bessel-DVR function. Furthermore, the use of the $N_1 N_2 L$ special points within Method II requires only a single summation, see eqn (21). A highly special feature of Method II is that it employs different grid points corresponding to the different basis functions for determination of the potential energy matrix elements. Overall, Method II is about $N_2 L$ times less expensive than Method I. For the largest calculations presented this means close to three orders of magnitude saving when building V^K. Therefore, we advocate the use of Method II in further applications. Similarly to direct-product DVRs, in Method II the overall cost of the nuclear motion calculation is determined solely by the cost of obtaining the desired eigenvalues and eigenfunctions.

The relatively widely known implicitly restarted Arnoldi method has been used to obtain the eigenvalues of the nonsymmetric Hamiltonian resulting from the use of Method II. Within this method, during the matrix-vector multiplications advantage can easily be taken of the sparsity and special structure of the Hamiltonian. The implicitly restarted Arnoldi algorithm proved very stable in all test computations. Further refinement of the iterative determination of eigensolutions might make Method II even more appealing for nuclear motion computations when the goal is the determination of the full rotational–vibrational spectrum.

The results obtained during this study show that a basis-function-dependent grid is accurate and efficient though this GFBR results in a nonsymmetric Hamiltonian matrix. As the numerical tests suggest, all the at least nearly converged eigenvalues of this Hamiltonian have zero imaginary parts. The new algorithm easily results in converged rotational–vibrational energy levels, for example, for X_3 species above the barrier to linearity. As a test of the algorithm, $J = 2$ rotational–vibrational energy levels of H_3^+ have been pre-sented. The eigenenergies obtained by the new method, based on the use of a nondirect-product basis within Methods I and II, are compared to converged results computed by a simple technique,[31,32] which does not treat the radial singularities but uses the Radau coordinate system. For H_3^+, the use of the Radau Hamiltonian with a DOPI-like algorithm can be advocated for determining eigenenergies perhaps up to about 30 000 cm^{-1} above the ZPE.

References

1 See, for example, the special issue of *Spectrochim. Acta*, 2002, **58A**.
2 M. J. Bramley and T. Carrington, Jr, *J. Chem. Phys.*, 1993, **99**, 8519.
3 I. N. Kozin, M. N. Law, J. M. Hutson and J. Tennyson, *J. Chem. Phys.*, 2002, **118**, 4896.
4 (a) M. J. Bramley and N. C. Handy, *J. Chem. Phys.*, 1993, **98**, 1378; (b) S. Carter, N. Pinnavaia and N. C. Handy, *Chem. Phys. Lett.*, 1995, **240**, 400.
5 D. Luckhaus, *J. Chem. Phys.*, 2003, **118**, 8797.
6 M. Mladenović, *Spectrochim. Acta*, 2002, **58A**, 795.
7 H.-G. Yu, *J. Chem. Phys.*, 2002, **117**, 2030.
8 H.-G. Yu, *J. Chem. Phys.*, 2003, **120**, 2270.
9 O. L. Polyansky, A. G. Császár, S. V. Shirin, N. F. Zobov, P. Barletta, J. Tennyson, D. W. Schwenke and P. J. Knowles, *Science*, 2003, **299**, 539.
10 J. Tennyson, N. F. Zobov, R. Williamson, O. L. Polyansky and P. F. Bernath, *J. Phys. Chem., Ref. Data*, 2001, **30**, 735.
11 T. Furtenbacher, A. G. Császár and J. Tennyson, *J. Mol. Spectrosc.*, 2007, accepted for publication.
12 B. T. Sutcliffe, *J. Chem. Soc., Faraday Trans.*, 1993, **89**, 2321.
13 (a) I. Last, M. Gilibert and M. Baer, *J. Chem. Phys.*, 1997, **107**, 1451; (b) M. Baer, G. Niedner-Schatteburg and J. P. Toennies, *J. Chem. Phys.*, 1989, **91**, 4169; (c) M. Baer, G. Niedner-Schatteburg and J. P. Toennies, *Chem. Phys. Lett.*, 1990, **167**, 269.
14 (a) J. K. G. Watson, *Can. J. Phys.*, 1994, **72**, 702; (b) J. K. G. Watson, *Chem. Phys.*, 1995, **190**, 291.
15 J. R. Henderson, J. Tennyson and B. T. Sutcliffe, *J. Chem. Phys.*, 1993, **98**, 7191.
16 S. Carter and W. Meyer, *J. Chem. Phys.*, 1990, **93**, 8902.
17 V. Spirko, A. Cejhan and P. Jensen, *J. Mol. Spectrosc.*, 1987, **134**, 430.
18 (a) J. R. Henderson and J. Tennyson, *Chem. Phys. Lett.*, 1990, **173**, 133; (b) J. R. Henderson and J. Tennyson, *Mol. Phys.*, 1996, **89**, 953; (c) J. J. Munro, J. Ramanlal, J. Tennyson and H. Y. Mussa, *Mol. Phys.*, 2006, **104**, 115; (d) P. Barletta, B. C. Silva, J. J. Munro and J. Tennyson, *Mol. Phys.*, 2006, **104**, 2801.
19 H. Zhang and S. C. Smith, *J. Chem. Phys.*, 2005, **123**, 014308.
20 (a) M. J. Bramley, J. W. Tromp, T. Carrington, Jr and G. C. Corey, *J. Chem. Phys.*, 1994, **100**, 6175; (b) M. J. Bramley, G. C. Corey and I. P. Hamilton, *J. Chem. Phys.*, 1995, **103**, 9705.
21 V. A. Mandelshtam and H. S. Taylor, *J. Chem. Soc., Faraday Trans.*, 1997, **93**, 847.
22 X. T. Wu and E. F. Hayes, *J. Chem. Phys.*, 1997, **107**, 2705.
23 J. C. Light, I. P. Hamilton and J. V. Lill, *J. Chem. Phys.*, 1985, **82**, 1400.
24 D. O. Harris, G. G. Engerholm and W. D. Gwinn, *J. Chem. Phys.*, 1965, **43**, 1515.

3414 | *Phys. Chem. Chem. Phys.*, 2007, **9**, 3407–3415

This journal is © the Owner Societies 2007

25 A. S. Dickinson and P. R. Certain, *J. Chem. Phys.*, 1968, **49**, 4209.
26 V. Szalay, G. Czakó, Á. Nagy, T. Furtenbacher and A. G. Császár, *J. Chem. Phys.*, 2003, **119**, 10512.
27 V. Szalay, *J. Chem. Phys.*, 1996, **105**, 6940.
28 J. R. Henderson and J. Tennyson, *Comput. Phys. Commun.*, 1993, **75**, 365.
29 J. Tennyson, M. A. Kostin, P. Barletta, G. J. Harris, O. L. Polyansky, J. Ramanlal and N. F. Zobov, *Comput. Phys. Commun.*, 2004, **163**, 85.
30 B. T. Sutcliffe and J. Tennyson, *Int. J. Quantum Chem.*, 1991, **39**, 183.
31 G. Czakó, T. Furtenbacher, A. G. Császár and V. Szalay, *Mol. Phys.*, 2004, **102**, 2411.
32 T. Furtenbacher, G. Czakó, B. T. Sutcliffe, A. G. Császár and V. Szalay, *J. Mol. Struct.*, 2006, **780–781**, 283.
33 J. Tennyson and B. T. Sutcliffe, *J. Mol. Spectrosc.*, 1983, **101**, 71.
34 B. R. Johnson, *J. Chem. Phys.*, 1980, **73**, 5051.
35 M. Vincke, L. Malegat and D. Baye, *J. Phys. B: At. Mol. Opt. Phys.*, 1993, **26**, 811.
36 M. Hesse, *Phys. Rev. E*, 2002, **65**, 046703.
37 G. Czakó, V. Szalay, A. G. Császár and T. Furtenbacher, *J. Chem. Phys.*, 2005, **122**, 024101.
38 R. G. Littlejohn, M. Cargo, T. Carrington, Jr, K. A. Mitchell and B. Poirier, *J. Chem. Phys.*, 2002, **116**, 8691.
39 R. G. Littlejohn and M. Cargo, *J. Chem. Phys.*, 2002, **117**, 27.
40 G. Czakó, V. Szalay and A. G. Császár, *J. Chem. Phys.*, 2006, **124**, 014110.
41 D. C. Sorensen, *SIAM J. Matr. Anal. Appl.*, 1992, **13**, 357.
42 http://www.caam.rice.edu/software/ARPACK/.
43 (*a*) R. Radau, *Ann. Sci. Ec. Normale Super.*, 1868, **5**, 311; (*b*) F. T. Smith, *Phys. Rev. Lett.*, 1980, **45**, 1157.
44 C. Leforestier, *J. Chem. Phys.*, 1991, **94**, 6388.
45 (*a*) V. Szalay, *J. Chem. Phys.*, 1993, **99**, 1978; (*b*) D. Baye and P.-H. Heenen, *J. Phys. A: Math. Gen.*, 1986, **19**, 2041.
46 C. Lanczos, *J. Res. Natl. Bur. Stand.*, 1950, **45**, 255.
47 O. L. Polyansky, R. Prosmiti, W. Klopper and J. Tennyson, *Mol. Phys.*, 2000, **98**, 261.
48 J. Tennyson, M. A. Kostin, H. Y. Mussa, O. L. Polyansky and R. Prosmiti, *Philos. Trans. Royal Soc. London, Ser. A*, 2000, **358**, 2419.
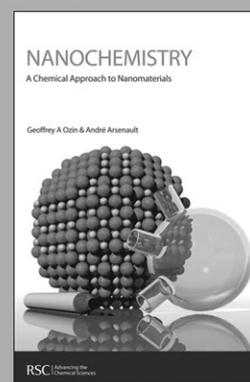
This journal is © the Owner Societies 2007

Phys. Chem. Chem. Phys., 2007, **9**, 3407–3415 | 3415